Proceedings of the VIII International Conference ION 2010, Kazimierz Dolny, Poland, June 14–17, 2010

Stopping Power and Energy Straggling of Channeled He-Ions in GaN

A. Turos[a,b,*], R. Ratajczak[b], K. Pągowska[b], L. Nowicki[b], A. Stonert[b] and P. Caban[a]

[a]Institute of Electronic Materials Technology, Wólczyńska 133, 01-919 Warsaw, Poland

[b]Sołtan Institute of Nuclear Studies, 05-400 Otwock/Świerk, Poland

GaN epitaxial layers are usually grown on sapphire substrates. To avoid disastrous effect of the large lattice mismatch a thin polycrystalline nucleation layer is grown at 500 °C followed by the deposition of thick GaN template at much higher temperature. Remnants of the nucleation layer were visualized by transmission electron microscopy as defect agglomeration at the GaN/sapphire interface and provide a very useful depth marker for the measurement of channeled ions stopping power. Random and aligned spectra of He ions incident at energies ranging from 1.7 to 3.7 MeV have been measured and evaluated using the Monte Carlo simulation code McChasy. Impact parameter dependent stopping power has been calculated for channeling direction and its parameters have been adjusted according to experimental data. For virgin, i.e. as grown, samples, the ratio of channeled to random stopping power is constant and amounts to 0.7 in the energy range studied. Defects produced by ion implantation largely influence the stopping power. For channeled ions the variety of possible trajectories leads to different energy loss at a given depth, thus resulting in much larger energy straggling than that for the random path. Beam energy distributions at different depths have been calculated using the McChasy code. They are significantly broader than those predicted by the Bohr formula for random direction.

PACS: 61.82.Fk, 61.85.+p, 68.55.Ln, 68.35.Dv

1. Introduction

The Rutherford backscattering/channeling (RBS/c) is one of the most frequently used techniques for depth profiling and defect analysis. However, important errors can appear if the appropriate stopping power has not been applied for the depth conversion. It is well known that the stopping power for channeled ions is significantly lower than that of non-channeled ions. Experimental and theoretical analysis of stopping power in the channeling mode is a complex task because of many effects involved, like: impact parameter dependence of energy loss, variety of possible ion trajectories, and atomic electron density distribution models.

There is a relatively large number of papers addressed to this issue, however, they are almost exclusively focused on the channeling in Si [1–6]. Typically energy loss measurements have been performed in the transmission mode by measuring the final energy of ions transmitted through self-supported thin single crystals. The principal drawback of this method lies in the preparation of homogeneous thin crystals with perfect surfaces. Because of difficulties in fulfillment of this requirement this technique has been abandoned nowadays. Alternatively, single crystals or epitaxial layers of usually perfect crystalline quality can be used for the purpose provided they contain a depth marker embedded in the structure. Such a marker can be the rear edge of upper crystalline layer in a SIMOX structure [1, 2, 5] or thin layer doped with a heavy element in a heterostructure of Si(doped)/Si type [6]. Also resonant elastic scattering has been used, where the shift of the resonance position is an indication of changes in stopping power [3]. Data on the stopping power measurement in semiconductor compound crystals are rather scarce [7, 8]. These reports are either old or are rather side products of different research than the results of a systematic study. In this report, results of stopping power measurements in GaN epitaxial layers are presented.

Since GaN single crystals are hardly available the most commonly used substrates for GaN epitaxy are sapphire (Al_2O_3) and SiC. Because of the great lattice mismatch the structure of grown layers is far from being perfect. As grown defects are typically misfit dislocations originated at the interface with the density decreasing with the layer thickness. Device structures (transistors and lasers) are grown on several μm thick GaN epilayers called templates. Ion channeling has been applied for GaN analysis for more than two decades [9, 10]. There are two energy regions of interest for RBS/c applications: the first one around 2 MeV is typically used for analysis of ion implan-

* corresponding author; e-mail: Andrzej.Turos@itme.edu.pl

tation produced defects and results are restricted to the Ga-sublattice, the second one located at 3.7–4.2 MeV allows N-sublattice analysis using non-Rutherford scattering. It has been demonstrated that the ^{14}N(^{4}He, ^{4}He)^{14}N elastic scattering cross section resonance at 3.7 MeV can be used for N profiling both in random and channeling mode [11].

The modified Monte Carlo simulation code McChasy has been applied to spectra analysis and stopping power calculations [12, 13].

2. Experimental

Samples were prepared using metal-organic vapor phase epitaxy (MOVPE) technique in the Aixtron AX100HTRD reactor at Institute of Electronic Materials Technology, Warsaw. The GaN films were deposited onto 2 inch diameter (0001) sapphire wafers. A standard two-step deposition process was employed [14, 15]. The substrate was first heated before the growth in H_2 at high temperature then after cooling up to the temperature of 500 °C AlN nucleation layer of approximately 60 nm thickness was deposited. Subsequently, the wafer was heated to 1050 °C for deposition of 300–8000 nm thick GaN films. Trimethylgalium TMGa and ammonia NH_3 were used as Ga and N source, respectively. Purified hydrogen was used as the carrier gas.

Ion implantation was performed at room temperature (RT) with 320 keV Ar ions to fluences ranging from 2×10^{12} to 1×10^{17} at./cm^2. Virgin and implanted samples were analyzed with RBS/c using 1.7–3.7 MeV ^{4}He-ions from Van de Graaff and Tandetron accelerators at the Institute for Ion Beam Physics and Materials Research Forschungszentrum Dresden, Germany. Complementary structural analysis was performed by transmission electron microscopy (TEM) using Jeol JEM 3010 electron microscope operating at 300 kV. Cross-section TEM specimens were prepared by a standard method of mechanical pre-thinning followed by Ar ion milling.

3. Results and discussion

Figure 1 shows random and aligned RBS spectra for 1160 nm thick virgin GaN epilayer measured at 3.7 MeV incident ^{4}He-ion energy. In the random spectrum the broad peak at high energies is due to the scattering by Ga atoms. The scattering on Al atoms in AlN nucleation layer produces the peak around 1000 keV, overlapping with the continuous spectrum produced by the scattering from the sapphire substrate. Channeling spectrum along [0001] axis revealed a very low channeling minimum yield, $\chi_{\min} \leq 2\%$. The large peak in aligned spectrum around 2000 keV is due to defect agglomeration, mostly misfit dislocations, located in the vicinity of GaN/sapphire interface. TEM observations revealed in this region an irregular tangle of dislocations, loops, stacking faults and other defects. Detailed defect depth distributions have been calculated using the McChasy code assuming that defects are randomly displaced Ga and N atoms. The best fit to the experimental spectrum has been obtained for defect distribution consisting of a rectangular peak containing 25 at.% of displaced atoms covering the depth interval of 100 nm located in the GaN layer next to the sapphire substrate. The quality of such a fit can be seen in Fig. 2. Very low channeling $\chi_{\min}$ in the near surface region is due to the fact that, according to the TEM analysis, threading dislocations originated in this region are predominantly of screw or mixed type with the Burgers vector along (0001) direction. Such defects do not obstruct ion motion and are practically "invisible" for channeling ions along (0001) axis.

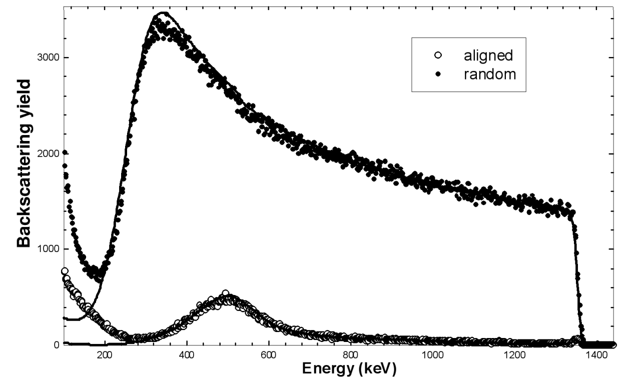

Fig. 1. Random and [0001] aligned spectra for 1160 nm thick GaN epitaxial layer for 1.7 MeV incident ^{4}He-ion energy.

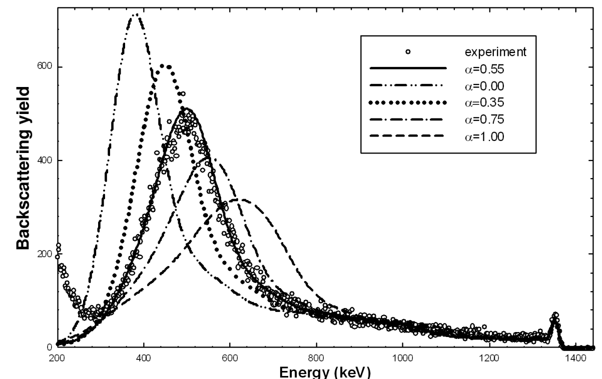

Fig. 2. Aligned spectrum for 1160 nm thick GaN epitaxial layer for 1.7 MeV incident ^{4}He-ion energy. Damage peak due to misfit defects at the GaN/sapphire interface is located in the low energy part of the spectrum. Adjustment of channeled ions stopping power for correct location of misfit defects peak has been performed by calculating of aligned spectra for different values of α using the McChasy code.

Presence of defect group at a well defined depth provides a very useful depth marker for the adjustment of channeled ions stopping power, S_{ch}. Classical Lindhard [16] approach has been applied for local energy loss; in this approach the energy loss of channeled particle is

a sum of two terms: the first one is proportional to the local electron density, being hence impact parameter dependent and the second one is random stopping power. In the McChasy code $S_{\rm ch}$ is defined as

$$S_{\rm ch} = \alpha S_{\rm l} + (1-\alpha) S_{\rm r} \,, \qquad (1)$$

where $S_{\rm r}$ — random stopping power, $S_{\rm l}$ — local stopping power (cf. Ref. [9] for calculation details), α is a free parameter ($0 \le \alpha \le 1$). Figure 2 shows calculated aligned spectra for different values of α. The correct location of damage peak has been obtained for $\alpha = 0.55$.

Figure 3 shows depth variation of the calculated stopping power in virgin GaN crystals for different value of the parameter α and two incident He ion energies: 1.7 MeV and 3.7 MeV. The wiggles of channeled stopping power in first 300 nm are due to flux density fluctuations. They reflect the quasi-coherent oscillatory motion of channeled ions at shallow depth and disappear with increasing depth where the flux statistical equilibrium has been attained. As can be easily calculated from z data shown in Fig. 2 the ratio of channeled to random stopping power is constant and amounts to 0.7 in the energy range studied.

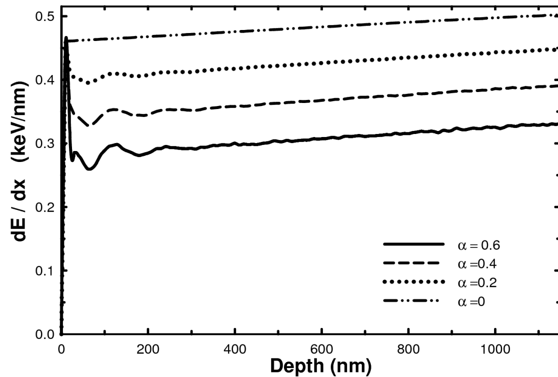

Fig. 3. Calculated stopping power for ^{4}He ions in GaN as a function of depth for various parameters α and incident energy 1.7 MeV.

Figure 4 shows depth variation of the calculated stopping power in GaN bombarded to different fluences of 320 keV Ar ions. Structural defects alter the flux distribution and have a pronounced influence on the stopping power. Results of our recent study of the defect buildup in GaN due to Ar-ion implantation has been published elsewhere [17]. Defect distributions produced by 320 keV Ar-ion bombardment extend over 300 nm and the increase of their concentration follows the three-step accumulation model [18]. The dependences of α and stopping power on the defect concentration are shown in Fig. 5. Increase of defect concentration causes continuous increase of stopping power from the value characteristic for virgin crystal ($\alpha = 0.55$) to that of amorphous compound ($\alpha = 0$) producing shift of the marker peak (cf. Fig. 2). Moreover, even the local increase of stopping power in the depth interval 80–300 nm reflecting the damage depths distribution can be well reproduced in the Monte Carlo simulations as can been seen in Fig. 3.

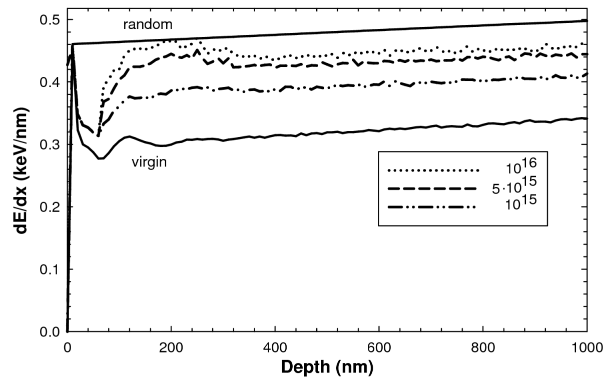

Fig. 4. Calculated stopping power as a function of depth for 1.7 MeV ^{4}He ions in GaN bombarded to different fluences of 320 keV Ar ions.

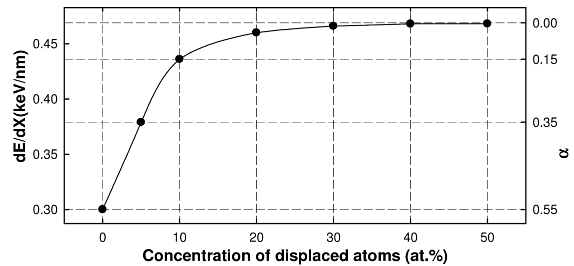

Fig. 5. Stopping power for 1.7 MeV ^{4}He ions in GaN as a function of damage concentration. Corresponding stopping power parameter α is shown on the right hand axis.

TABLE

Dependence of the straggling FWHM ($\Delta E_{\rm s}$) for 1.7 MeV incident ^{4}He ions on defect concentration produced by 320 keV Ar-ion bombardment.

Fluence [at./cm^2]	Maximum defect concentration [%]	$\Delta E_{\rm s}$ at 300 nm [keV]	$\Delta E_{\rm s}$ at 600 nm [keV]	$\Delta E_{\rm s}$ at 900 nm [keV]
0	0	28	58	95
1×10^{15}	5	21	40	59
5×10^{15}	10	13	26	39
1×10^{16}	>50	13	26	39

Detailed inspection of the width of simulated marker peaks in Fig. 2 reveals another important feature of the particle trajectory dependent energy loss. The peak for $\alpha = 0$ (random) is significantly narrower than that for $\alpha = 1$ (hyperchanneling). In fact the energy spread of channeled ions is significantly greater than that for random direction. This is primarily due to the great variety

of trajectories of channeled ions. Following different trajectories ions penetrate regions of different electron density resulting in a large energy spread at a given depth. Detailed results are shown in Table where FWHMs of ion energy distributions (ΔE_s — straggling width) at different depths are listed. Moreover, the straggling width evolution due to different defect concentrations is also given. One notes that for $\alpha = 0$ the straggling width is that of random i.e. of amorphous sample. It should be added that such values estimated for 3.7 MeV beam at similar conditions follow the same tendency and are larger by 20% only.

4. Conclusions

It is generally accepted that the energy loss of channeled ions is principally due to the interaction with valence electrons that are uniformly distributed across the channel. At high enough ion energy the ratio of channeled to random stopping power decreases due to additional contribution of interaction of non-channeled ions with core, more specifically L-shell, electrons. However, for the energy range of interest these electrons cannot be excited by well channeled ions because the small enough impact parameters are inaccessible for them. Hence, the stopping power ratio becomes independent of energy and its value reflects to some degree the distribution of valence electrons across the channel. This is the case for the (0001) channel in the hexagonal GaN structure and explains our observation of energy independent ratio of channeled to random stopping power in the 1.7–3.7 MeV energy range.

Our results have demonstrated that for correct channeling analysis of GaN epitaxial layers the stopping power for channeled ions has been applied that strongly depends on the defect distribution in the analyzed crystal. The depth resolution of the RBS/c technique is strongly influenced by channeled beam straggling, which can be significantly greater than the random value. Moreover, beam density fluctuations at shallow depth can also influence the accuracy of analysis. All these effects are hardly accessible for analytical or semiempirical methods. Only using dedicated Monte Carlo simulation codes like McChasy the experimental spectra can be accurately reproduced and evaluated.

Acknowledgments

This work was supported by the Polish Ministry of Science and Higher Education, grant No. N 51502931/1104. We thank J. Borysiuk for TEM analysis.

RBS/c analysis has been carried out at AIM of the Institute of Ion Beam Physics and Materials Research of Forschungszentrum Dresden–Rossendorf within the framework of the specific research and technological development programme of the European Community "Structuring the European Research Area: Research Infrastructures Transnational Access" (RITA contract No. 025646). Helpful assistance of R. Groetzschel and F. Munnik is warmly acknowledged.

References

[1] J.H.R. dos Santos, P.L. Grande, H. Boudinov, M. Behar, R. Stoll, Chr. Klatt, S. Kalbitzer, *Nucl. Instrum. Methods Phys. Res. B* **106**, 51 (1995).

[2] R. Greco, A. Luce, Y. Wang, L. Shao, *Nucl. Instrum. Methods Phys. Res. B* **261**, 538 (2007).

[3] E. Kotai, *Nucl. Instrum. Methods Phys. Res. B* **118**, 43 (1996).

[4] E. Kotai, *Nucl. Instrum. Methods Phys. Res. B* **148**, 172 (1999).

[5] Y. Yamamoto, A. Ikeda, T. Yoneda, K. Kajiyama, Y. Kido, *Nucl. Instrum. Methods Phys. Res. B* **153**, 10 (1999).

[6] Lin Shao, Y.Q. Wang, M. Nastasi, J.W. Mayer, *Nucl. Instrum. Methods Phys. Res. B* **249**, 51 (2006).

[7] D.W. Hetherington, *Nucl. Instrum. Methods Phys. Res. B* **115**, 319 (1996).

[8] Y. Yamamoto, J. Kaczanowski, Y. Kido, J. Nakata, H. Yamaguchi, K. Takahei, *Phys. Rev. A* **53**, 1644 (1996).

[9] A. Turos, L. Nowicki, A. Stonert, M. Leszczyński, I. Grzegory, S. Porowski, *Mater. Sci. Forum* **248-249**, 419 (1997).

[10] B. Holländer, S. Mantl, M. Mayer, C. Kirchner, A. Pelzman, M. Kamp, S. Christiansen, M. Albrecht, H.P. Strunk, *Nucl. Instrum. Methods Phys. Res. B* **136-138**, 1248 (1998).

[11] A. Turos, R. Ratajczak, K. Pągowska, A. Stonert, L. Nowicki, P. Caban, *Nucl. Instrum. Methods Phys. Res. B* **266**, 1897 (2008).

[12] A. Dygo, A. Turos, *Phys. Rev. B* **40**, 7704 (1989).

[13] L. Nowicki, A. Turos, R. Ratajczak, A. Stonert, F. Garrido, *Nucl. Instrum. Methods Phys. Res. B* **240**, 277 (2005).

[14] X.H. Wu, D. Kapolnek, E.J. Tarsa, B. Heying, S. Keller, B.P. Keller, U.K. Mishra, S.P. DenBaars, J.S. Speck, *Appl. Phys. Lett.* **68**, 1371 (1996).

[15] M. Kamp, *Opt. Quantum Electron.* **32**, 227 (2000).

[16] J. Lindhard, *Mat. Fys. Medd. K. Dan. Vidensk. Selsk.* **34**, 1 (1965).

[17] K. Pągowska, R. Ratajczak, A. Stonert, A. Turos, *Acta Phys. Pol. A* **120**, 153 (2011).

[18] J.J. Jagielski, L. Thomé, P. Aubert, O. Maciejak, A. Piatkowska, R. Groetzschel, *Nucl. Instrum. Methods Phys. Res. B* **266**, 2902 (2008).